

Axions++ 2023 Workshop



Josep Maria Batllori Berenguer

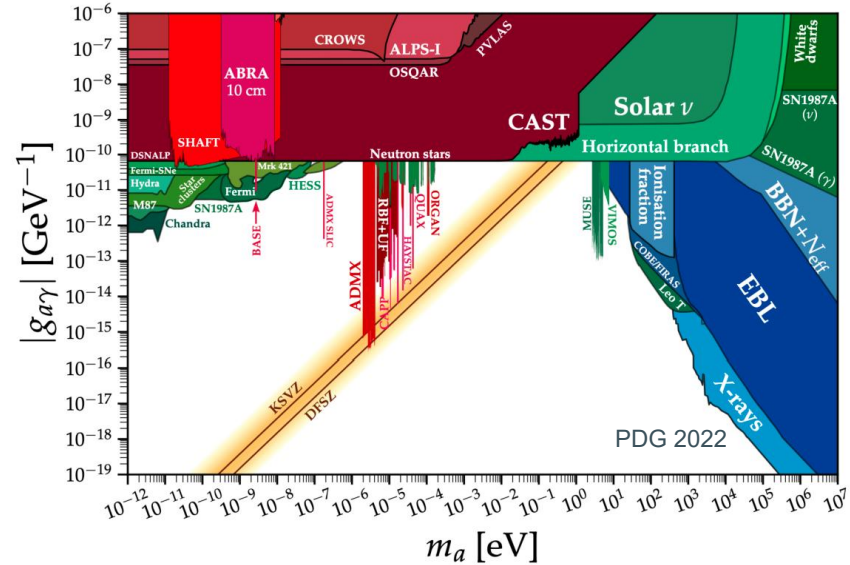
Working Group: J. M. Batllori, Y. Gu, D. Horns, M. Maroudas, J. Ulrichs

WISPF1: WISP Searches on a Fiber Interferometer



Motivation

- **Axions** solve the strong CP problem and are prominent candidates for CDM [1].
- Haloscope experiments are very sensitive in μeV but depend on the **local DM density** \rightarrow poorly constrained \rightarrow could be substantially smaller [2].
- LSTW experiments are not sensitive to QCD axions (conversion scales with $g^4_{a\gamma\gamma}$).
- **High axion mass range** (meV to eV) is unexplored by direct detection experiments (except CAST [3]).
- Null results of direct DM searches \rightarrow Need for **novel approaches!**

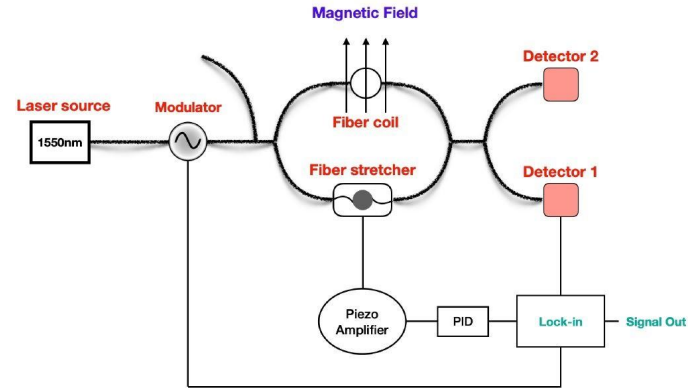


WISPFI (WISP searches on a Fiber Interferometer)

<https://doi.org/10.48550/arXiv.2305.12969>

- Novel table-top experiment focusing on **photon-axion conversion** in a waveguide by measuring **photon disappearance** in the presence of a strong external B field [4].
- Axion conversion probability scales with [5]:
For $P_{\gamma \rightarrow a} \ll 1$: $P_{\gamma \rightarrow a} \propto g_{a\gamma\gamma}^2 (BL)^2$
- Light guiding over **long distances & resonant detection** at a specially-confined region inside the bore of a strong magnet.
- **Mach-Zehnder interferometer** with the sensing arm inside the magnetic field.
- Expected signal: **amplitude reduction & phase shift**.

- No local DM density dependence.
- Operation at room temperature (no cryogenic setup required).



Photon-axion conversion

$$P_{\gamma \rightarrow a} = \underbrace{\sin^2(2\theta)}_{\text{Amplitude}} \underbrace{\sin^2(\pi L/L_{osc})}_{\text{Oscillations}} \quad [6] \quad \text{Mixing angle: } \tan(2\theta) = 2\omega \frac{g_{a\gamma\gamma} B}{k_\gamma^2 - k_a^2} \quad \leftarrow \text{Photon, axion wave momenta}$$

- Maximum conversion occurs for **large energy ω** or at $\mathbf{k}_\gamma = \mathbf{k}_a$ (resonant conversion, $\theta = 45^\circ$).
- Axion mass at resonance in a medium with effective refractive index n_{eff} :

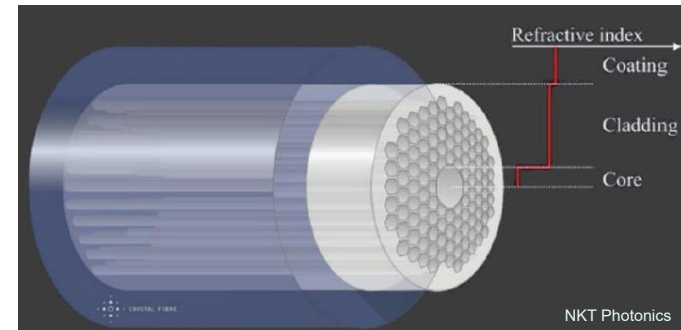
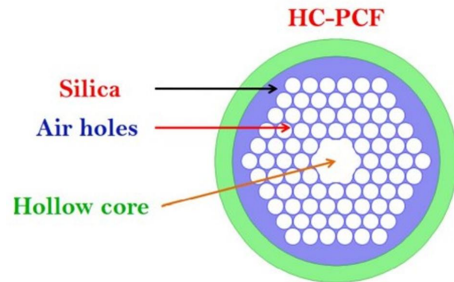
$$m_a = \omega \sqrt{1 - n_{eff}^2} \quad \longrightarrow \quad \text{Required } n_{eff} < 1!$$

- For $P_{\gamma \rightarrow a} \ll 1$ the resulting probability becomes: $P_{\gamma \rightarrow a} \approx 10^{-18} \left(\frac{g_{a\gamma\gamma}}{10^{-12} \text{ GeV}^{-1}} \right)^2 \left(\frac{B}{10 \text{ T}} \right)^2 \left(\frac{L}{200 \text{ m}} \right)^2$


 Energy (ω) independent!

Hollow-Core Photonic Crystal Fibers (HC-PCF)

- Resonant conditions can not be fulfilled for wave-guides based on dielectric materials.
- HC-PCF guide light through a low-refractive index hollow core which is surrounded by a periodic arrangement of air-holes in the cladding this generating a photonic-bandgap structure [7].
- Through the bandgap structure, the propagating mode can acquire $n_{\text{eff}} < 1$ leading to real axion masses and resonant mixing.

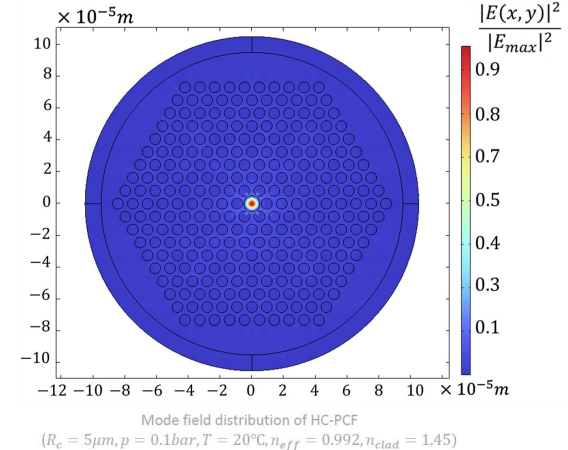


Effective mode index in HC-PCF (I)

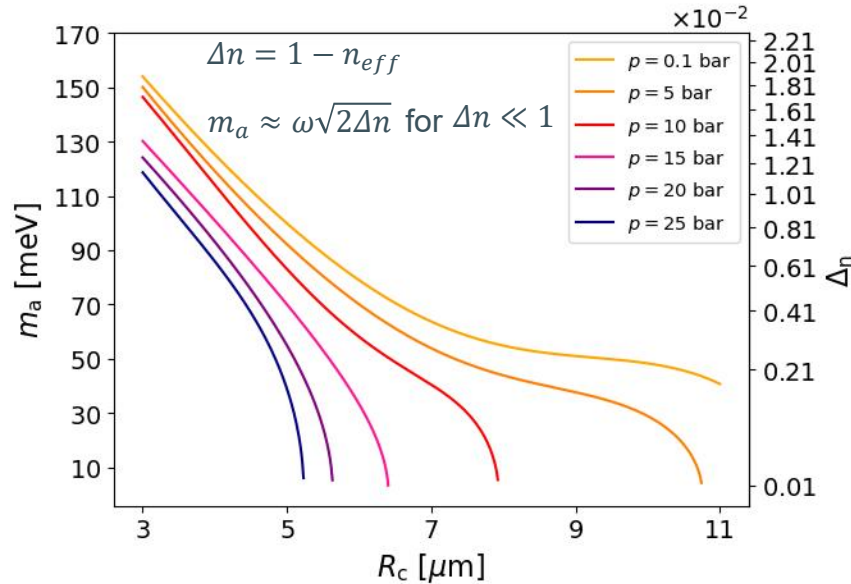
- n_{eff} depends on the core radius (R_c), the bending radius (R_b), and the refractive index of the effective gas (n_{gas}) which in turn depends on pressure (p), wavelength (λ), and temperature (T) [8, 9].

- Analytical approximation [8]:
$$n_{\text{eff}} = \frac{k_\gamma}{k_o} = \sqrt{n_{\text{gas}}^2(\lambda, p, T) - \left(\frac{u_{nm}}{k_\gamma R_c}\right)^2}$$

- FEM simulations studying the actual fiber geometry.



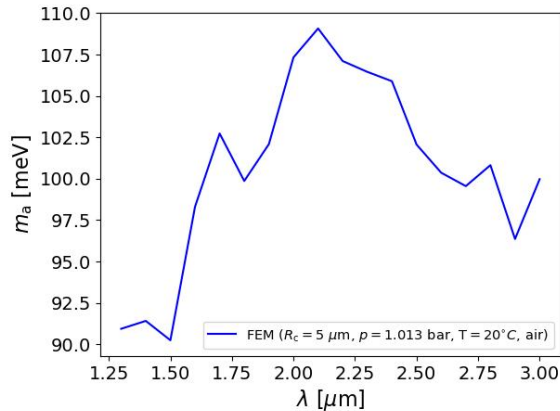
Effective mode index in HC-PCF (II)



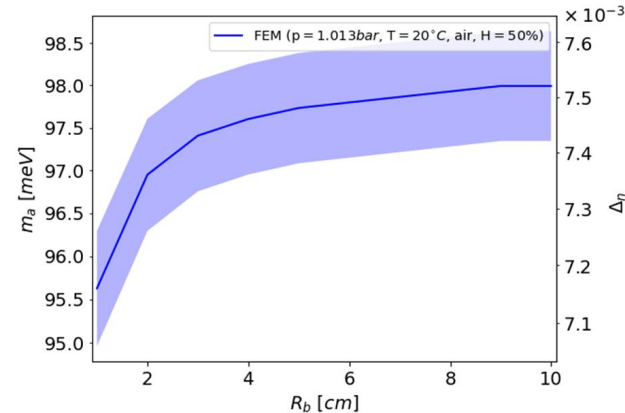
- Probed axion masses for resonant conversion based on different core radii (R_c) and pressures (p) of the air that fill the hollow core vary between ~ 10 meV to **160 meV**.
- Observed increase of n_{eff} with increasing R_c and p matches the analytical approximation.

Effective mode index in HC-PCF (III)

- Wavelength of the propagating light and bending radius of the fiber also have an effect on the effective mode index.



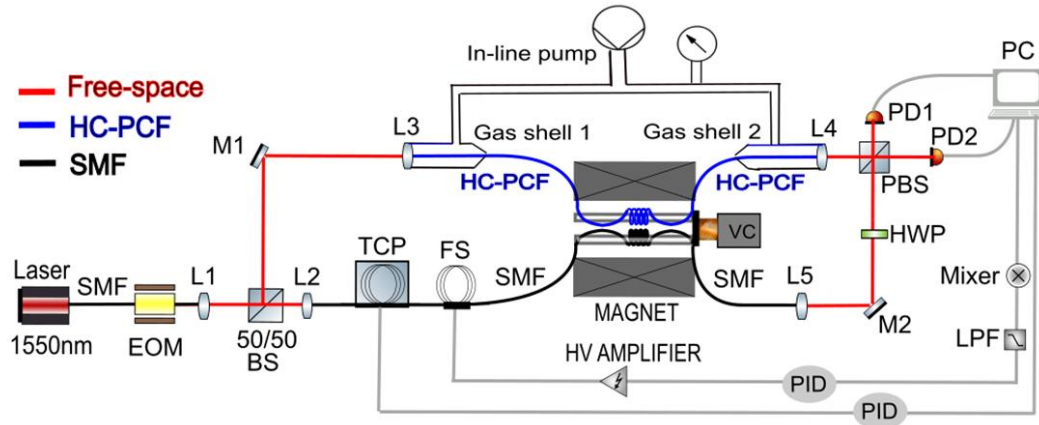
$$\Delta n = 1 - n_{eff} \quad m_a \approx \omega \sqrt{2\Delta n}$$



$$n'_{gas}(\lambda, \rho, T) = n_{gas}(\lambda, \rho, T) * n_{bend} = n_{gas}(\lambda, \rho, T) * \left(1 + \frac{R_c}{R_b}\right)$$

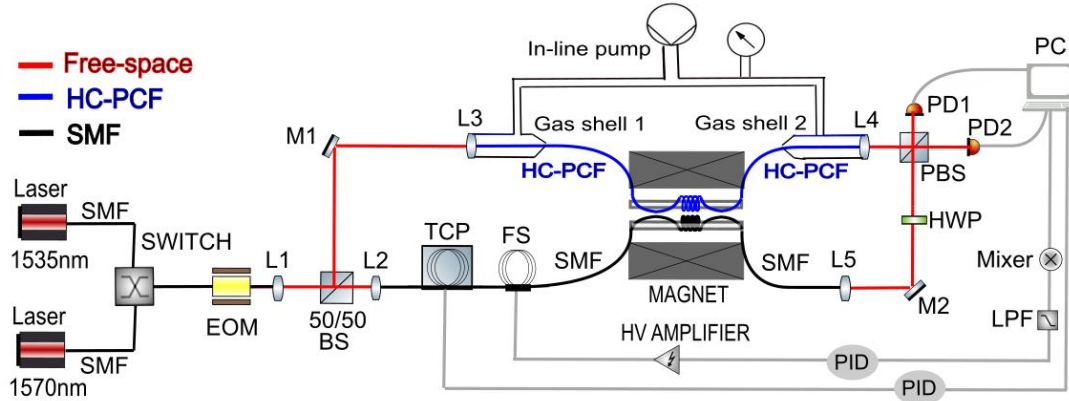
Experimental setup (I) - Voice coil modulation

- Partial free space partial fiber Mach-Zehnder-type interferometer.
- Sensing arm by HC-PCF placed in the magnetic bore and pressurized for tuning the probed axion mass.
- Both arms mounted on a **voice coil (VC)** for modulating the axion signal by shifting the position of the fiber coils and thus changing the effective B field.
- Fiber stretcher (FS) and temperature control pad (TCP) used for locking the interferometer via a PID.



Experimental setup (II) - wavelength switch modulation

- Partial free space partial fiber Mach-Zehnder-type interferometer.
- Sensing arm by HC-PCF placed in the magnetic bore and pressurized for tuning the probed axion mass.
- Both arms mounted on the bore of the magnet. The axion signal is modulated by **optically switching** two wavelengths of the input lasers beams (1535nm & 1570nm).
- Fiber stretcher (FS) and temperature control pad (TCP) used for locking the interferometer via a PID.

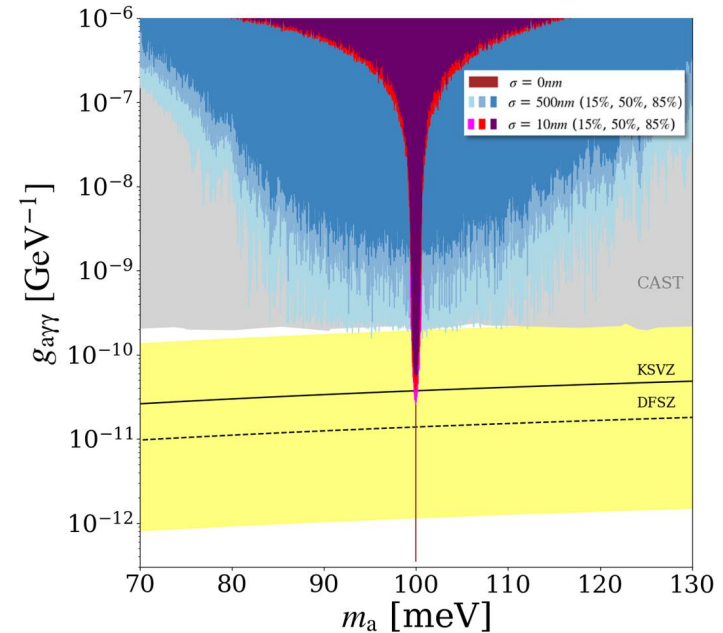


Sensitivity (I)

- MZI operated at dark fringe.
- Instrumental noise dominated by the dark current of the photo-detector.
- No additional losses.

$$g_{a\gamma\gamma} \approx 4 \times 10^{-13} \text{GeV}^{-1} \left(\frac{SNR}{3}\right)^{1/2} \left(\frac{B}{14T}\right)^{-1} \left(\frac{L}{500m}\right)^{-1} \left(\frac{P_{tot}}{4W}\right)^{-1/2} \left(\frac{\beta_{sig}}{1}\right)^{-1/2} \left(\frac{t}{180d}\right)^{-1/4} \left(\frac{NEPPD}{0.5fW/\sqrt{Hz}}\right)^{1/2}$$

- Axion mass mainly depends on core radius (R_c)
- HC-PCF production process leads to random variations of the R_c which widen the probed axion mass range but reduce the sensitivity.



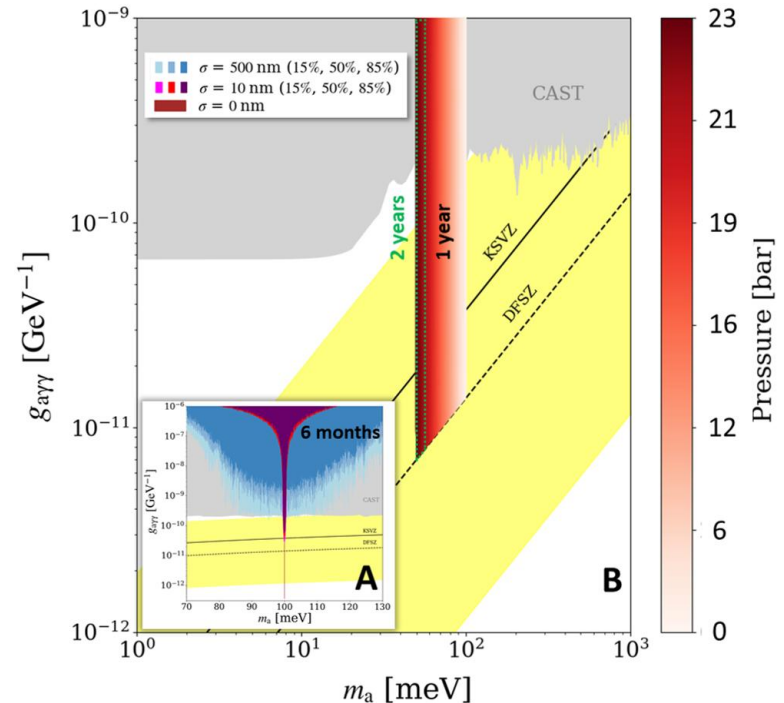
Sensitivity (II)

A. Baseline setup: 4 W laser @ 1550 nm,
 B = 14 T, 500 m HC-PCF at standard conditions.

B. Long term projection: 40 W laser @ 1550 nm,
 B = 14 T, 1 km PM HC-PCF with $\sigma=10$ nm.

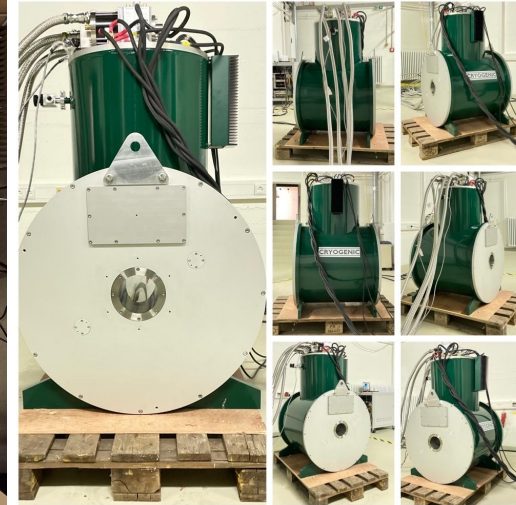
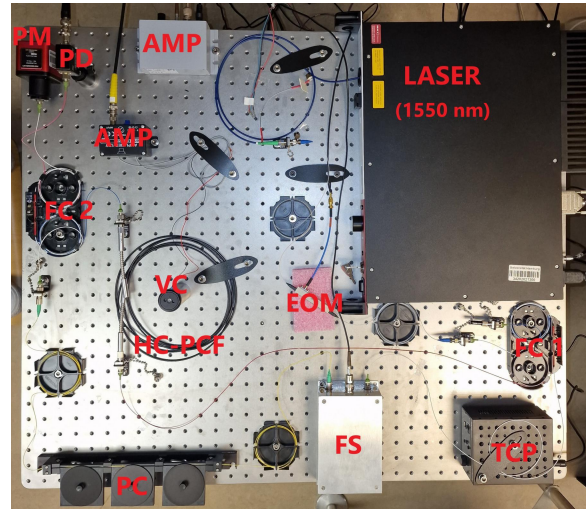
- Tuning from 0.1 – 23 bar in 116 steps of 0.6 meV between 50 – 100 meV

➔ **DFSZ sensitivity in a wide axion mass range!**



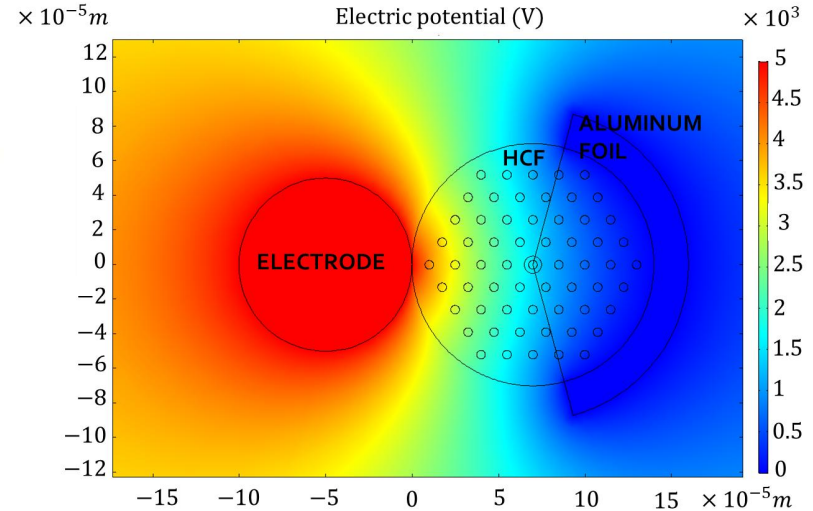
Future steps

- Test HC-PCF fiber in the 14 T warm-bore solenoid magnet.
- Signal modulation with VC / wavelength modulation.
- Interferometer locking in amplitude/phase and temperature for larger fiber lengths ($\sim 100\text{m}$).
- Integration to free-space (**ongoing**).
- Noise optimization.
- Final commissioning and data acquisition.
- Electric field conversion experiment (WISPFIE) using coaxial capacitor.

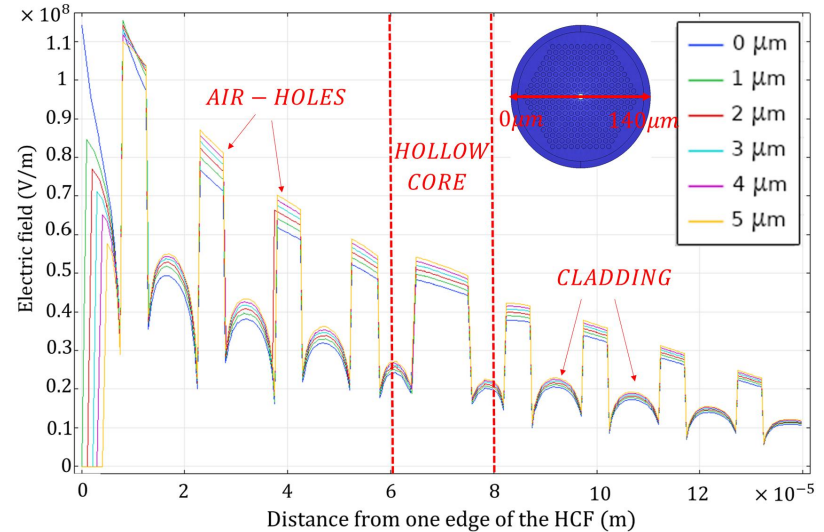
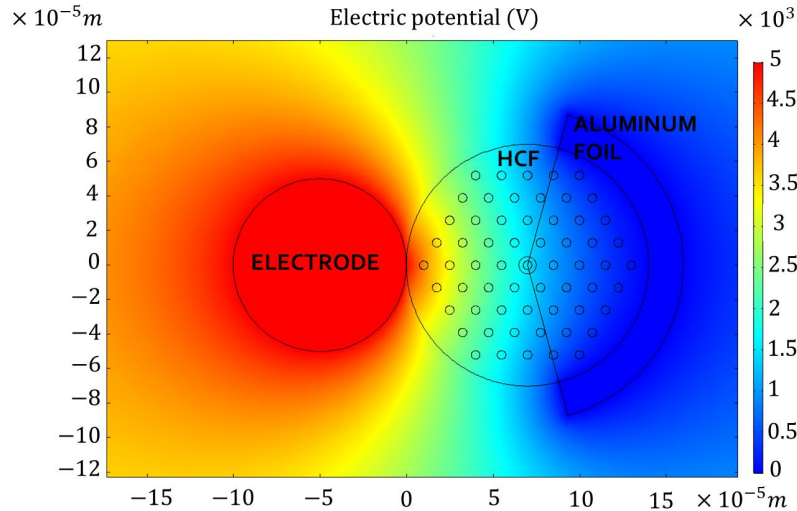


The axion-photon couplings g_{aAB} and g_{aBB} predicted in scenarios based upon modified Quantum-Electromagnetodynamics (QEMD) have not been exploited so far [6]. By attaching electrode strips to the HC-PCF, it is possible to probe the photon-axion conversion under the application and modulation of strong electric fields.

$$\begin{aligned}
 \nabla \times \mathbf{B}_a - \dot{\mathbf{E}}_a &= g_{aAA} (\mathbf{E}_0 \times \nabla a - \dot{a} \mathbf{B}_0) + g_{aAB} (\mathbf{B}_0 \times \nabla a + \dot{a} \mathbf{E}_0) , \\
 \nabla \times \mathbf{E}_a + \dot{\mathbf{B}}_a &= -g_{aBB} (\mathbf{B}_0 \times \nabla a + \dot{a} \mathbf{E}_0) - g_{aAB} (\mathbf{E}_0 \times \nabla a - \dot{a} \mathbf{B}_0) \\
 \nabla \cdot \mathbf{B}_a &= -g_{aBB} \mathbf{E}_0 \cdot \nabla a + g_{aAB} \mathbf{B}_0 \cdot \nabla a , \\
 \nabla \cdot \mathbf{E}_a &= g_{aAA} \mathbf{B}_0 \cdot \nabla a - g_{aAB} \mathbf{E}_0 \cdot \nabla a , \\
 (\partial^2 - m_a^2) a &= -(g_{aAA} - g_{aBB}) \mathbf{E} \cdot \mathbf{B} + g_{aAB} (\mathbf{E}^2 - \mathbf{B}^2) ,
 \end{aligned}$$



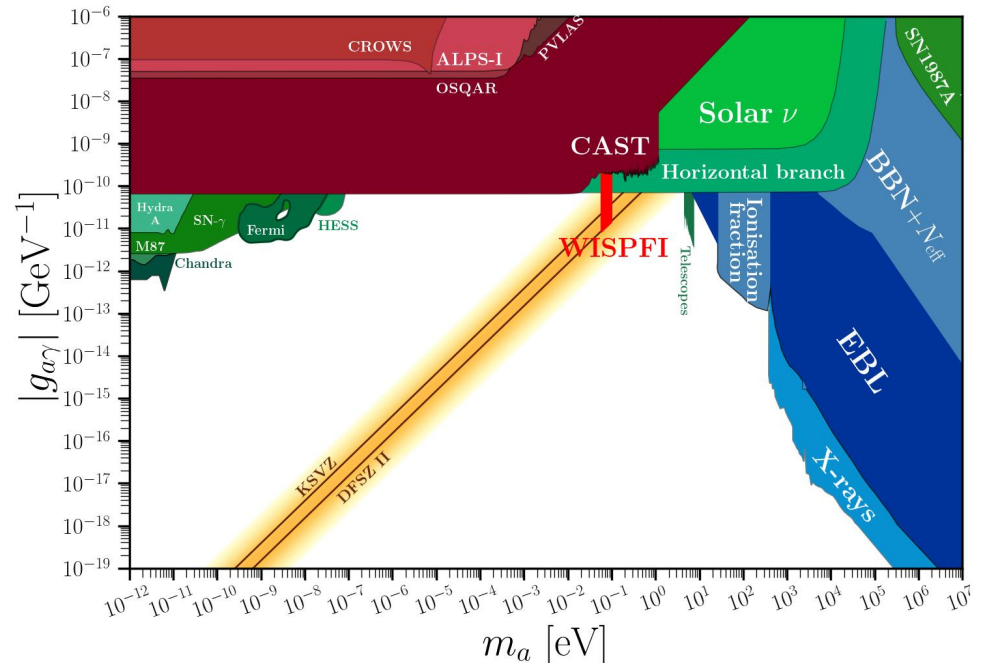
The axion-photon couplings g_{aAB} and g_{aBB} predicted in scenarios based upon modified Quantum-Electromagnetodynamics (QEMD) have not been exploited so far [6]. By attaching electrode strips to the HC-PCF, it is possible to probe the photon-axion conversion under the application and modulation of strong electric fields.



Summary

- Light guiding through **waveguide** embedded in a strong B field.
- Partial free-space, partial fiber **Mach-Zehnder**-type interferometer.
- **Amplitude/phase reduction/shift** in the presence of $\gamma \rightarrow a$ conversion.
- **HC-PCF** meets the conditions for resonant mixing.
- **Tuning** in a wide axion mass range by regulating the **gas pressure** in the fiber.

<https://doi.org/10.48550/arXiv.2305.12969>



Thanks for your attention!

**Find out more about the cluster:
www.qu.uni-hamburg.de**



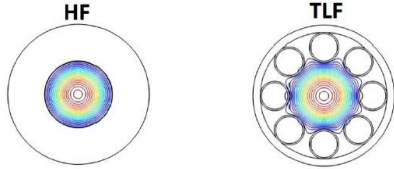
References

- (1) R. D. Peccei, H. R. Quinn, CP Conservation in the Presence of Pseudoparticles, Phys. Rev. Lett. 38, 1440 (1977), <https://doi.org/10.1103/PhysRevLett.38.1440>
- (2) B. Eggemeier et al., Axion minivoids and implications for direct detection, Phys. Rev. D 107, 083510 (2023), <https://doi.org/10.1103/PhysRevD.107.083510>
- (3) V. Anastssopoulos et al., New CAST limit on the axion-photon interaction, Nature Phys.13, 584-590 (2017), <https://doi.org/10.1038/nphys4109>
- (4) J. M. Batllori, et al, WISP Searches on a Fiber Interferometer under a Strong Magnetic Field, arXiv (2023), <https://doi.org/10.48550/arXiv.2305.12969>
- (5) H. Tam, Q. Yang, Production and detection of axion-like particles by interferometry, Phys. Lett. B, 716, 435-440 (2012), <https://doi.org/10.1016/j.physletb.2012.08.050>
- (6) G. Raffelt, L. Stodolsky, Mixing of the photon with low-mass particles, Phys. Rev. D 37, 1237 (1988), <https://doi.org/10.1103/PhysRevD.37.1237>
- (7) P. Russell, Photonic Crystal Fibers, Science 299, 5605 (2003), <https://doi.org/10.1126/science.1079280>
- (8) E. A. J. Marcatili, R. A. Schmelzter, Hollow Metallic and Dielectric Waveguides for Long Distance Optical Transmission and Lasers, Bell System Technical Journal 43, 4, (1964), <https://doi.org/10.1002/j.1538-7305.1964.tb04108.x>
- (9) L. Rosa et al., Analytical Formulas for Dispersion and Effective Area in Hollow-Core Tube Lattice Fibers, Fibers 9, 10, (2021), <https://doi.org/10.3390/fib9100058>
- (10) A. V. Sokolov and A. Ringwald, Electromagnetic Couplings of Axions (2022), arXiv (2023), <https://doi.org/10.48550/arXiv.2205.02605>

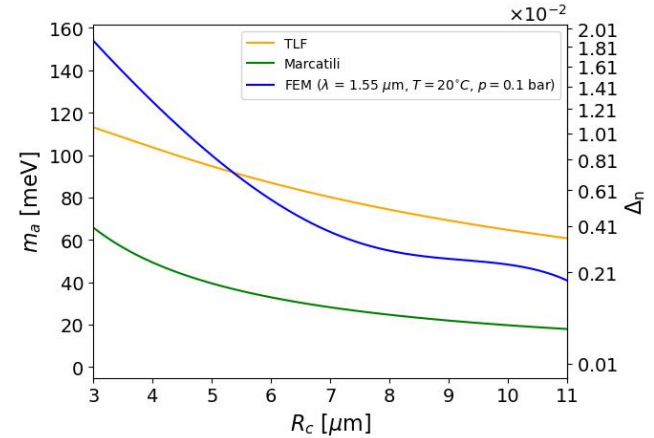
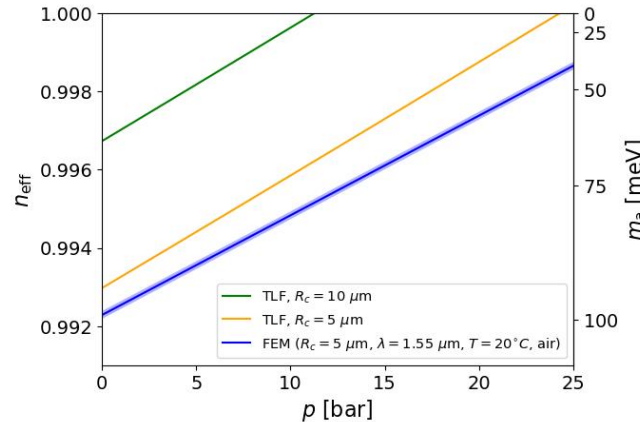


Backup Slides

Effective mode index in HC-PCF



$$n_{eff} = \frac{k_y}{k_o} = \sqrt{n_{gas}^2(\lambda, p, T) - \left(\frac{u_{nm}}{k_y R_c}\right)^2}$$



Refractive index of air

- Refractive index of air as a function of pressure and temperature for $T=20^{\circ}\text{C}$ and $P=1.013$ bar accordingly.

